Electronic Supplementary Material (ESI) for Environmental Science: Processes & Impacts.

Electronic Supplementary Information (ESI)

Direct and indirect photodegradation of atrazine and *S*-metolachlor in agriculturally impacted surface water and associated C and N isotope fractionation

Guillaume Drouin,[a] Boris Droz,*[a] Frank Leresche,[b] Sylvain Payraudeau,[a] Jérémy Masbou[a] and Gwenaël Imfeld*[a]

[a] Institut Terre et Environnement de Strasbourg (ITES), Université de Strasbourg/EOST/ENGEES, CNRS UMR 7063, 5 rue Descartes, Strasbourg F-67084, France.

[b] Department of Civil, Environmental, and Architectural Engineering, Environmental Engineering Program, University of Colorado Boulder, Colorado 80309, United States.

***Corresponding authors**

bodroz@bluewin.ch

imfeld@unistra.fr, + 333 6885 0474

This ESI includes 17 pages with texts, 5 tables and 6 figures.

Supporting materials and methods

List of chemicals and preparation of solutions

Pesticides. *S*-metolachlor (2-chloro-*N*-(2-ethyl-6-methylphenyl)-*N*-((2S)-1-methoxypropan-2-yl)acetamide), atrazine (6-chloro-4-*N*-ethyl-2-*N*-propan-2-yl-1,3,5-triazine-2,4-diamine) and metolachlor d_{11} were analytical grade (Pestanal, >99.9%, Sigma-Aldrich®, St Louis, MO, USA).

Transformation products of *S*-metolachlor and atrazine. *S*-metolachlor ethanesulfonic acid (ESA - sodium 2-((2-ethyl-6-methylphenyl)(1-methoxy-2-propanyl)amino)-2-oxoethanesulfonate), *S*-metolachlor oxanilic acid (OXA - 2-(2-ethyl*N*-(1-methoxypropan-2-yl)-6-methylanilino)-2-oxoacetic acid), metolachlor CGA 37735 (*N*-(2-ethyl-6-methylphenyl)-2-hydroxyacetamide), 2-hydroxy-atrazine (A-OH - 2-(ethylamino)-6-(propan-2-ylamino)-1*H*-1,3,5-triazin-4-one), desethylatrazine (DEA; 6-chloro-2-*N*-propan-2-yl-1,3,5-triazine-2,4-diamine), desisopropylatrazine (DIA; 6-chloro-2-*N*-ethyl-1,3,5-triazine-2,4-diamine), atrazine-desethyl2-hydroxy (A-DOH - (6*Z*)-4-Imino-6-(isopropylimino)-1,4,5,6-tetrahydro-1,3,5-triazin-2-ol) were analytical grade (>98%, Sigma-Aldrich®, St Louis, MO, USA). Hydroxy-metolachlor (Met-OH - *N*-(2-ethyl-6- methylphenyl)-2-hydroxy-*N*-(1-methoxypropan-2-yl)acetamide) was purchased as reference standard for GC in ACN from LGC Standards (Molsheim, France).

Actinometer. *p*-nitroanisole (PNA) and pyridine (anhydrous, >99.8%) were analytical grade (>97%).

Solvents and other chemicals: The solvents dichloromethane (DCM), acetonitrile (ACN) and ethyl acetate (EtOAc) were HPLC grade purity (>99.9%). All the pre-cited chemicals as well as magnesium sulfate heptahydrate (BioUltra, ≥99.5%), calcium chloride hexahydrate (BioUltra, ≥99.0%), calcium nitrate tetrahydrate (≥99.0%), potassium phosphate monobasic (BioUltra, ≥99.5%) and sodium phosphate dibasic (BioUltra, ≥99.5%) used for buffer solution and synthetic water preparation were purchased from Sigma-Aldrich® (St Louis, MO, USA).

Synthetic surface water:[1] Two 50 fold concentrated stock solutions, were prepared with (i) 3 mg L^{-1} $Ca(NO_3)_2 \cdot 4H_2O$, 15 mg L^{-1} $MgSO_4 \cdot 7H_20$, 20 mg L^{-1} $CaCl_2 \cdot 2H_2O$, and (ii) 30 mg L^{-1} $NaHCO_3$. (i) was dissolved into the require amount of ultrapure water, and (ii) was added undercontinuous stirring of the solution. Synthetic water was used after reaching equilibrium for CO_2 and constant pH (<24 hours). Synthetic water was filter-sterilized through 0.2 µm cellulose acetate (CA) syringe filter. Concentrations were control by triplicate measurement by ionic chromatography.

Table S1 Chemical composition of irradiation solutions

parameter	unit	value[a]	analytical method	irradiation solution
pH	-	7.9 ± 0.2	electrode	All
DOC[b]	mg L^{-1}	5.4 ± 0.2	TOC analyzer	SRFA & TOT
		cations		
NH_4^+		n.p.	IC	NIT & TOT
Na^+		9.9 ± 0.5	IC	NIT & TOT
K^+	mg L^{-1}	0.71 ± 0.04	IC	NIT & TOT
Mg^{2+}		1.47 ± 0.07	IC	NIT & TOT
Ca^{2+}		13.4 ± 0.7	IC	NIT & TOT
		anions		
Cl^-		12.0 ± 0.6	IC	NIT & TOT
NO_3^-	mg L^{-1}	20.5 ± 1.0	IC	NIT & TOT
SO_4^{2-}		5.6 ± 0.3	IC	NIT & TOT

[a] Analytical uncertainties reported correspond to one standard deviation over triplicate measurements. [b] DOC concentrations measured in UW were <0.2 mg C L^{-1}, which limited any effect of dissolved organic matter in direct photodegradation experiments (DIR and DIR254). n.p. not present, DOC: dissolved organic carbon.

Organic matter photobleaching

DOM photoirradiation reduces its light absorbance properties. The control experiment showed that the decrease of light absorbance at $\lambda = 254$ nm was less than 20% after >310 hours of irradiation. SRFA photosensitizing and light absorption effects were thus assumed constant across the experiments in TOT solutions. Also, the composition of SRFA did not changes over irradiation as evidenced by its steady absorption spectrum.

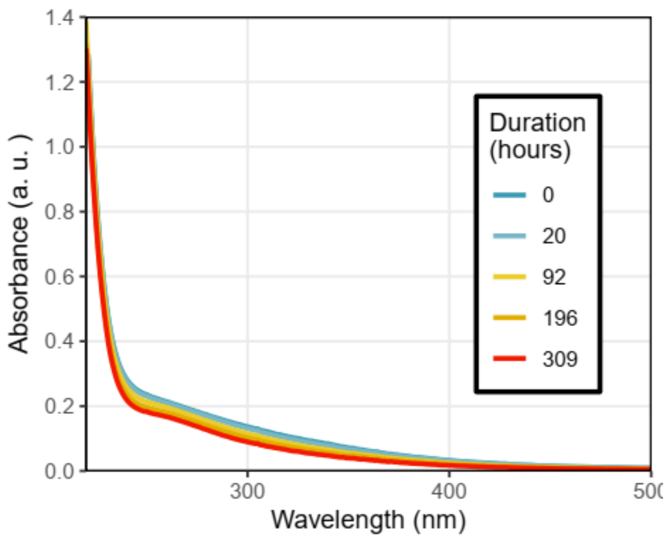

Fig. S1. Temporal changes of absorbance of the TOT solution caused by organic matter photobleaching.

PNA/Pyr actinometer system

A PNA (30 µM)/pyridine (10 mM) actinometer system was used to measure mean light intensity during experiments.[2, 3] Values of wavelength independent quantum yields (ϕ_{PNA}) of 3.19×10^{-3} mol E^{-1} were used from Laszakovits et al.[2] To account for a closed irradiation system (i.e., aluminium foil covering the quartz vial walls and assumed to reflect light without absorption), it was assumed that chemicals absorbed all of the incident light and the decay of PNA as expressed in eq. S1:[4]

$$\frac{dC_{PNA}}{dt}(\lambda) = \frac{\epsilon(\lambda)}{\sum_{\lambda}\epsilon(\lambda)} \times \phi_{PNA} \times F_W(\lambda) \qquad \text{(S1)}$$

with $\frac{dC_{PNA}}{dt}$ the observed pseudo first-order decaying rate of PNA, ϕ_{PNA} the wavelength independent PNA quantum yield, $\frac{\epsilon(\lambda)}{\sum_{\lambda}\epsilon(\lambda)}$ the relative fraction of light absorbed by PNA at wavelength λ also provided by Laszakovits et al.[2] and $F_W(\lambda)$ the relative photon irradiance of the lamp at wavelength λ.

$$\frac{dC_{PNA}}{dt} = \sum_{\lambda}\left(\frac{\epsilon(\lambda)}{\sum_{\lambda}\epsilon(\lambda)} \times \phi_{PNA} \times F_W(\lambda)\right) \qquad \text{(S2)}$$

eq. (and $F_W(\lambda)$ and $\frac{\epsilon(\lambda)}{\sum_{\lambda}\epsilon(\lambda)}$ were computed over the range of validity for the PNA/Pyr system $\lambda \in [290{,}400]$ nm.

Table S2 Irradiation conditions with Xenon arc lamp and correction factors used to estimate photodegradation rates.

light interval (Δλ)	VIS (360 < λ < 830 nm)		UVA (320 < λ < 400 nm)		UVB (280 < λ < 320 nm)		total (I_{tot})	correction factor[b]
Intensity[a]	absolute	relative	absolute	relative	absolute	relative	absolute	
	mW cm^{-2}	%	mW cm^{-2}	%	mW cm^{-2}	%	mW cm^{-2}	
experiment								
ATZ - DIR	16.4	68.4	6.8	28.3	0.8	3.4	24.0	0.63
ATZ - NIT	8.5	66.3	4.0	31.1	0.3	2.6	12.8	1.18
ATZ - SRFA	7.1	68.4	3.0	28.7	0.3	2.9	10.4	1.45
ATZ - TOT	12.9	64.1	6.7	33.4	0.5	2.5	20.2	0.75
SMET - DIR	13.1	68.0	5.6	28.9	0.6	3.1	19.3	0.78
SMET - NIT	6.2	70.5	2.4	27.1	0.2	2.4	9.9	1.52
SMET - SRFA	9.6	66.9	4.2	29.6	0.5	3.5	13.3	1.14
SMET - TOT	6.9	69.2	2.8	27.8	0.3	3.0	10.8	1.40
mean irradiation	10.1	67.7	4.4	29.4	0.4	2.9	15.1	
standard deviation	3.7	2.0	1.8	2.0	0.2	0.4	5.3	

[a] Light intensity are reported as the arithmetic mean of light measurements at the beginning and the end of the respective experiments. Relative light intensities stand for the contribution of each wavelength interval (VIS, UVA, UVB) to the whole irradiation, $I_{relative} = \frac{I_\lambda}{\sum_{i \in \{VIS,UVA,UVB\}} I_{\lambda_i}}$.

[b] Correction of degradation rates were performed according to the correction factors with the averaged total light intensity $\overline{I_{tot}}$ = 15.1 mW cm^{-2} as the reference value divided by individual total light intensities, $F_k = \overline{I_{tot}}/I_{tot}$.

Light spectrum homogeneity within the light-proof box

Light homogeneity within the light-proof box varied between 80 and 120% of relative irradiation intensity taking the mean intensity value as a reference. The LP Hg lamp was temporarily replaced by medium pressure Hg lamp emitting at λ = 365 nm and was used to irradiate 11 beakers filled with 50 mL of PNA (30 µM)/Pyridine (10 mM) actinometers and evenly distributed within the light-proof box. After four hours, the remaining concentration of PNA was measured in each beaker and the variations in the irradiation intensity were retrieved by comparing the mean value of k_{p_E} with individual values computed from eq. (S3.[2, 3]

$$\ln\left(\frac{[PNA]\,(t)}{[PNA]_0}\right) = k_{p_E} \times t \qquad \text{(S3)}$$

k_{p_E} stands for the pseudo first order reaction rate of PNA and is linearly proportional to the incident irradiance.

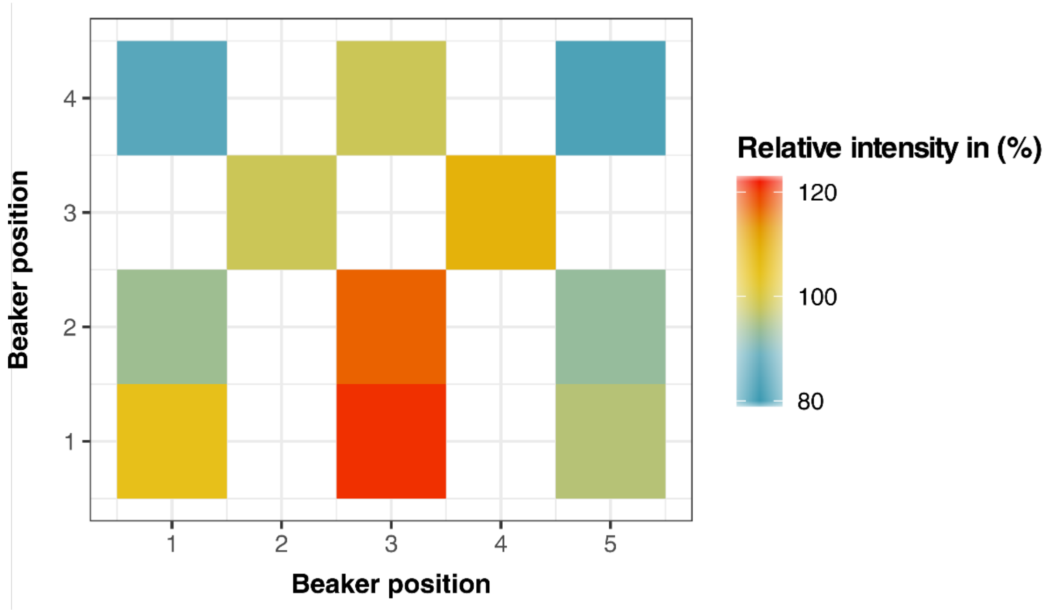

Fig. S2. Spatial distribution of irradiation intensity within the light-proof box. Transparent places correspond to empty spaces where the irradiation intensity was not measured within the light-proof box.

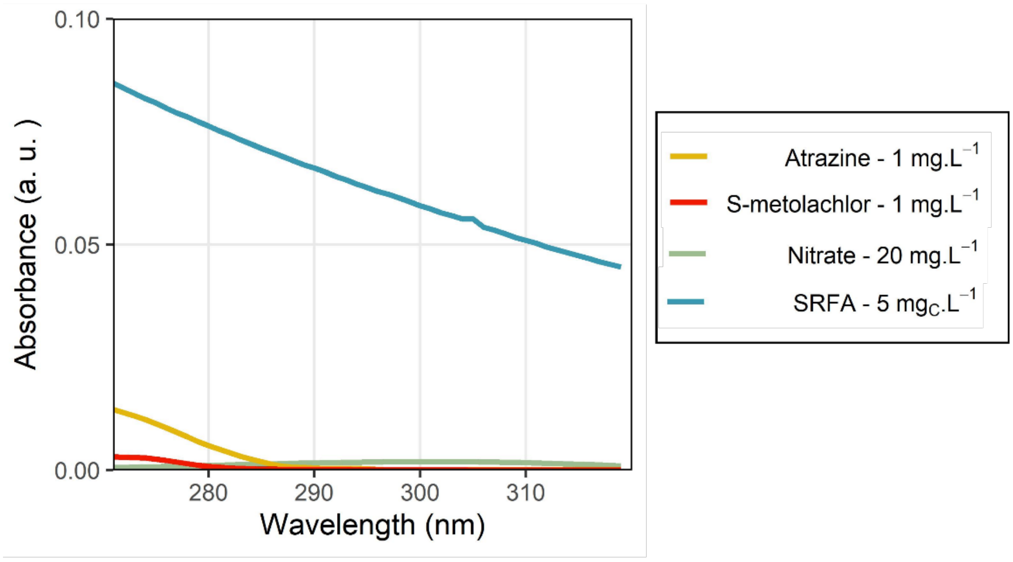

Fig. S3 UV-vis absorption spectra of atrazine, *S*-metolachlor, nitrates and SRFA at experimental concentrations. The absorption spectra for nitrates was extracted from Gaffney et al.[5]

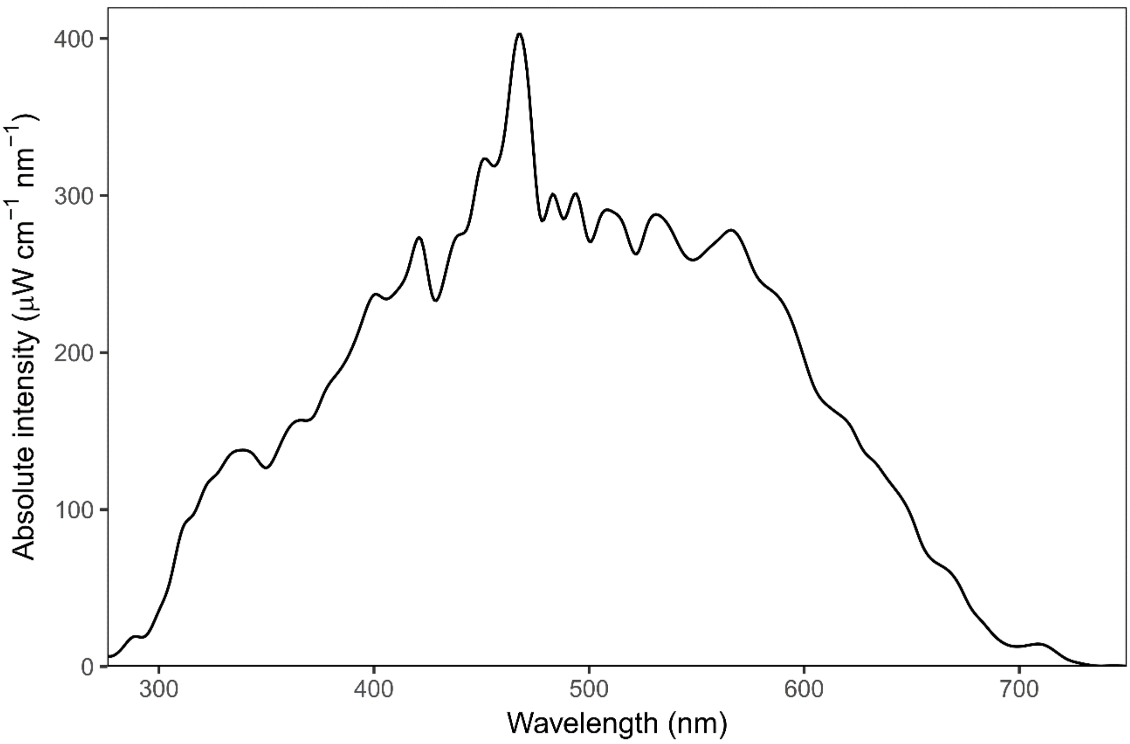

Fig. S4. Absolute light intensity as a function of the wavelength for the Xenon Arc Lamp as measured in the quartz tube after the liquid light guide. The light spectrum was characterized with a calibrated spectroradiometer ILT 900C (International Light®) at a wavelength resolution of 1 nm. Significant irradiation ($I(\lambda) > 0.1 \times I_{mean}$) ranged from [270;720] nm.

Table S3. Relative light intensity in function of the wavelength band for the low-pressure mercury lamp (LP Hg; P/N TUV G6T5, Phillips – nominal power 6W) use in the light-proof box (P/N 701 435, Jeulin).

λ (nm)	Spectral irradiance (arbitrary units)
253.7	100.0
313.0	3.3
365.5	3.8
404.7	4.8
435.8	6.9
546.1	5.7
578.0	4.1

Pesticide extraction, quantification and CSIA

Pesticide extraction

Solid phase extraction (SPE) on water samples was carried out using a SolEx C18 cartridges (1 g, Dionex®, CA, USA) and an AutroTrace 280 SPE system (Dionex®, CA, USA) as previously.[6] Briefly, SPE cartridges were sequentially rinsed with 5 mL of ethanol and ACN before being conditioned with 10 mL of deionized water. Liquid samples were then loaded at 10 mL min^{-1} and cartridges were dried afterwards under nitrogen flux for 10 minutes. Then, a sequential elution with 5 mL of EtOAc and ACN allowed pesticide elution before concentration up to the last droplet under nitrogen flux and resuspension in 1000 µL of ACN for storage at –20°C.

Pesticide quantification

Atrazine and *S*-metolachlor were quantified by gas-chromatography (GC, Trace 1300, Thermo Fisher Scientific) coupled with a mass-spectrometer (MS, ISQ™, Thermo Fisher Scientific) in selected-ion-monitoring mode. Each sample was injected twice to ensure analytical reproducibility and was diluted to fall within the linearity range of the MS, estimated according to the calibration curve to lie between 50 and 1000 µg L^{-1}. 1 µL of metolachlor d_{11} at 300 µg L^{-1} was systematically added to the 1 µL of sample as an Internal Standard (IS) by the autosampler (TriPlus RSH™, Thermo Fisher Scientific) and was used to normalize peak area of the molecules of interest. The combined 2 µL were then injected in split mode with a split flow of 6 mL min^{-1} at 280°C. Separation happened through a TG-5MS column (30 m × 0.25 mm ID, 0.25 µm film thickness) well suited for slightly polar molecules with a helium flow of 1.5 mL min^{-1}. Heat ramp started after 1 min at 50°C and raised up to 160°C at a rate of 30°C min^{-1}, continued up to 220°C at 4°C min^{-1} and finally reached 300°C at 30°C min^{-1} to be held for 1 min. The MS transfer line and the source were kept at 320°C for the entirety of the analysis. Detection limits (DLs) and quantification limits (QLs) were estimated on multiple injection method and are 4 and 30 µg L^{-1} respectively.[7]

Transformation products quantification

Transformation products were analysed in samples displaying similar extent of degradation (≈ 80%). The general methodology followed Villette et al. (2019)[8] and is summarized below. Samples were analyzed by a Dionex Ultimate 3000 (Thermo-Fischer Scientific, USA) liquid chromatograph (LC) coupled to an Impact-II (Bruker, Germany) quadrupole time of flight (Q-TOF) high resolution mass spectrometer (HR-MS/MS). Molecule fragments generated during positive and negative ionization were scanned over a range of 30 to 1000 m/z with a resolving power of 54,000 defined at 400 m/z. Molecule identification was performed by comparison with a list of mass spectra of potential transformation products extracted from the literature. Identified structures were confirmed by matching retention times (RT <0.2 min) and exact mass spectra of commercially available analytical standards.

C and N CSIA of atrazine and *S*-metolachlor

A GC-C-IRMS device fitted with a TRACE™ ultra gas chromatograph (ThermoFisher Scientific) coupled via a GC IsoLink/Conflow IV interface to an Isotope Ratio Mass Spectrometer (DeltaV plus, ThermoFisher Scientific) allowed for measurements of carbon and nitrogen isotope composition of atrazine and *S*-metolachlor following established method.[9] Samples were injected in split mode with a split flow of 30 mL min^{-1} at 250°C. For both atrazine or *S*-metolachlor, chromatographic separation happened through a TG-5MS column (60 m × 0.25 mm ID, 0.25 µm film thickness) with helium as the carrier gas at a flow rate of 1.5 mL min^{-1} according to the following method. The heat ramp started after 1 min at 50°C and raised up to 150°C at a rate of 15°C min^{-1}, continued up to 250°C at 2°C min^{-1} and finally reached 300°C at 20°C min^{-1} to be held for 3 min. The oxidation oven consisted of a single combined reactor (P/N 1255321, NiO tube and CuO-NiO-Pt wires, Thermo Fischer Scientific) and was set at 1000°C. A cold finger filled with liquid nitrogen trapped CO_2 formed during the combustion for N measurements. Measurements were systematically carried out within the linearity range for C and N.

Prediction of degradation rates and identification of dominant photodegradation processes

The effective contribution of nitrates and DOM as photosensitizers can be inferred from eq. S4. The observed degradation rates were composed of the sum of elemental photo-oxidation processes (e.g., direct, HO• and $^3DOM^*$ mediated).[10-12] The contribution of carbonate radicals ($CO_3^{\bullet-}$) as potential relevant photosensitizer was not included here because Vionne et al.[13] highlighted the limited oxidation of atrazine and anilines with $CO_3^{\bullet-}$ under sunlight irradiation even in carbonate rich waters (sum of [HCO_3^-] and [CO_3^{2-}] ≈ 10 times higher than in our conditions).[13] Accordingly, eq. S4 can be simplified to eq. S5. However, carbonates were considered as significant quenchers of HO•.[10]

$$\frac{dC}{dt} = -k_{obs} \times C \tag{S4}$$

$$\frac{dC}{dt} = -\Big(k_{dir} + k_{HO\bullet} \times [HO\bullet]_{SS} + k_{^3DOM^*} \times [^3DOM^*]_{SS} + k_{CO_3^{\bullet-}} \times [CO_3\bullet^-] + k_{^1O_2} \times [^1O_2]_{SS}\Big) \times C$$

$$\frac{dC}{dt} = -\Big(k_{dir} + k_{HO\bullet} \times [HO\bullet]_{SS} + k_{^3DOM^*} \times [^3DOM^*]_{SS} + k_{^1O_2} \times [^1O_2]_{SS}\Big) \times C \tag{S5}$$

C stands for pesticide concentration, k_{obs} for the observed degradation rate (s^{-1}), which is expressed as the sum of direct (k_{dir}) and selected indirect processes ($k_{HO\bullet}$, $k_{^3DOM^*}$, $k_{^1O_2}$). The latter degradation rates are second order and depend on the steady state concentrations of the associated short-lived reactive intermediates ($[^3DOM^*]_{ss}$, $[^1O_2]_{ss}$ and $[HO\bullet]_{ss}$).

Calculation of short-lived reactive intermediates steady state concentrations

Estimating the steady state concentrations of short-lived reactive intermediates requires identification of the main photosensitizers promoting and scavenging radicals and short-lived species and to determine the amount of light absorbed by each photosensitizers. The latter step accounts for competition for light irradiance between the different light-absorbing dissolved species as well as corrections for light attenuation.

Identification of main photosensitizers

Main short-lived reactive intermediates involved in pesticide photodegradation ($^3DOM^*$, $^1O_2$ and HO•) were formed through photosensitizer irradiation, respectively fulvic substances and nitrates.[14] $^3DOM^*$ and $^1O_2$ originates from irradiation of DOM and HO• from irradiation of DOM and nitrates.[3] Fulvic acids such as SRFA also have the ability to scavenge HO• and $^1O_2$.[15, 16] These species are short-lived and their concentrations in water are balanced by their ratio of production over quenching as expressed in eq.S6, S7 and S8.[4]

$$[HO\bullet]_{SS} = S(\lambda) \times \frac{\Phi_{HO\bullet,NO_3^-} \times k_{a,NO_3^-} \times [NO_3^-] + \Phi_{HO\bullet,DOM} \times k_{a,DOM} \times [DOM]}{k_{HO\bullet,DOM} \times [DOM] + k_{HO\bullet,HCO_3^-} \times [HCO_3^-] + k_{HO\bullet,CO_3^{2-}} \times [CO_3^{2-}]} \tag{S6}$$

$$[^1O_2]_{SS} = S(\lambda) \times \frac{\Phi_{^1O_2,DOM} \times k_{a,^1O_2} \times [DOM]}{k_{d,^1O_2}} \tag{S7}$$

$$[^3DOM^*]_{SS} = S(\lambda) \times \frac{\Phi_{^3DOM^*,DOM} \times k_{a,DOM} \times [DOM]}{k_{^3DOM^*,O_2} \times [O_2]} \quad \text{(S8)}$$

$\Phi_{\mathrm{R,Sens}}$ refers to the quantum yield of formation of short-lived reactive intermediates (R) by the photosensitizer (Sens) expressed in mol E^{-1}, $k_{a,Sens}$ stands for the rate constant of light absorption by Sens over the whole light spectrum considered and is expressed in E mol^{-1} s^{-1} and $k_{R,Sens}$ is the second-order rate constant of consumption of R by Sens in mol^{-1} L s^{-1}. $k_{d,^1O_2}$ refers to the first-order reaction rate of $^1O_2$ with water and is expressed in s^{-1}. $[O_2]$ was set to 2.4×10^{-4} M corresponding to the aqueous saturation at 20°C. $S(\lambda)$ refers to the light screening factor developed in eq.S9 below.

Although it is in principle possible to evaluate $[^3DOM^*]_{ss}$ using eq. S8, there are some uncertainties in the literature about the value of $\Phi_{^3DOM^*}$. We chose to evaluate $[^3DOM^*]_{ss}$ using the following expression: $[^3DOM^*]_{ss} \approx [^1O_2]_{ss} / f_\Delta$, where f_Δ is the fraction of $^3DOM^*$ that produces $^1O_2$. We chose a value of 0.34 for f_Δ based on data for a Suwannee River natural organic matter isolate from the IHSS.[17]

Second-order rate constant for the reaction between atrazine or *S*-metolachlor and $^3DOM^*$ can be found in Zeng et al.[10] They were determined by multiplying measured pseudo-first order reaction constant by the estimated $[^3DOM^*]_{ss}$. As the $[^3DOM^*]_{ss}$ reported in Zeng et al.[10] were manifestly underestimated (it does not follow the expression $[^3DOM^*]_{ss} \approx [^1O_2]_{ss} / f_\Delta$), it was necessary to correct the reported constant by recalculating them. We achieved that by recalculating $[^3DOM^*]_{ss}$ in Zeng et al.[10] Then we calculated the corrected second-order rate between atrazine or *S*-metolachlor and $^3DOM^*$ as the reported second-order rate constant divided by the recalculated $[^3DOM^*]_{ss}$ and multiplied by the reported $[^3DOM^*]_{ss}$

Table S4 Kinetic parameters for formation and consumption of short-lived reactive intermediates.

		units	ref.
quenching rates			
$k_{HO\cdot,DOM}$	1.6×10^{8}	$M^{-1}s^{-1}$	A
$k_{HO\cdot,HCO_3^-}$	1×10^{7}	$M^{-1}s^{-1}$	B
$k_{HO\cdot,HCO_3^{2-}}$	4×10^{8}	$M^{-1}s^{-1}$	B
$k_{^3DOM^*,O_2}$	2×10^{9}	$M^{-1}s^{-1}$	C
$k_{d,^1O_2}$	1.5×10^{5}	s^{-1}	C, D
quantum yield of formation			
$\Phi_{HO\cdot,NO_3^-}$	1×10^{-2}	-	E
$\Phi_{HO\cdot,DOM}$	1.65×10^{-5}	-	F
$\Phi_{^3DOM^*,DOM}$	4.2×10^{-4}	-	F
$\Phi_{^1O_2,DOM}$	6.54×10^{-2}	-	F
second-order rate constants for reactions			
atrazine			
$k_{HO\cdot,atr}$	2.7×10^{9}	$M^{-1}s^{-1}$	G
$k_{^1O_2,atr}$	2.0×10^{5}	$M^{-1}s^{-1}$	G
$k_{^3DOM^*,atr}$	1.2×10^{9}	$M^{-1}s^{-1}$	G
S-metolachlor			
$k_{HO\cdot,met}$	6.9×10^{9}	$M^{-1}s^{-1}$	G
$k_{^1O_2,met}$	4.4×10^{5}	$M^{-1}s^{-1}$	G
$k_{^3DOM^*,met}$	9.8×10^{8}	$M^{-1}s^{-1}$	G

Ref. A[15], B[13,18], C[12], D[16,19], E[20], F[21], G.[10]

Calculation of light absorption rates and light screening factors

Calculations were performed over the spectral range $\lambda \in [270 - 320$ nm$]$ as it corresponds to the range of significant absorbance for all dissolved species with respect to the emission spectrum of the Xenon arc lamp. As the light path length changed over repetitive samplings, an average path length of 15 cm was chosen as representative across the experiments. Changes in the actual path length would only significantly affect the absolute predicted degradation rates while the relative contribution of different processes would remain unaffected. The light screening factor ($S(\lambda)$) was computed in its wavelength dependent form. We assumed the light to travel straight through the quartz vial and to be insensitive to light scattering as in eq. S9.[22] Depending on the water composition, $Sens_i$ referred to a combination of DOM, NO_3^-, atrazine and *S*-metolachlor. We introduced $S(\lambda)$ to calculate the rate of light absorption as shown in eq. S10.[10]

$$S(\lambda) = \frac{1 - e^{-2.303 \times \sum(\epsilon_i(\lambda) \times [Sens]_i) \times l}}{2.303 \times \sum(\epsilon_i(\lambda) \times [Sens]_i) \times l} \quad \text{(S9)}$$

$$k_{a,Sens} = \sum S(\lambda) \times \frac{A_i(\lambda)}{A_{tot}(\lambda)} \times E_0 \times (1 - 10^{-A_{tot}(\lambda)}) \quad \text{(S10)}$$

Correction of ε_{bulk} accounting for repetitive sampling

The stepwise correction proposed by Buchner et al.[23] was adapted to non-volatile pesticide to evaluate if ε_{bulk} should account for repetitive sampling. This method consists of correcting the non-degraded fraction ($f = C(t) / C(t = 0)$) of atrazine or *S*-metolachlor at each sampling time (t). First, the individual f for two consecutive sampling times is calculate ($f_{(t-1)\to t}$). This fraction represents the amount (n) change due to the transformation only between by comparing the amount in the system before ($t - 1$) and at time t:

$$f_{(t-1)\to t} = \frac{n_w(t)}{n_w(t-1) - n_{rem}(t-1)} = \frac{C_w(t) \times V_w(t)}{C_w(t-1) \times V_w(t-1) - C_w(t-1) \times V_{rem}(t-1)} \quad \text{(S11)}$$

where n_W and n_{rem} correspond to the amount of the pesticide in the bulk water of the experiment and the amount removed by sampling at a given time t respectively. The amount is calculated by multiplying the concentration in the bulk water phase (C_w) with the bulk volume (V_w) or the removed volume (V_{rem}).

Second, the overall substrate fraction (f_{SW}) at time t is calculated considering $f(0)$ = 1 (i.e., 100% of the pesticide amount) and the eq. S11 for all sampling steps:

$$f_{SW}(t) = f(0) \times f_{t0\to t1} \times f_{t1\to t2} \times \cdots \times f_{t(n-1)\to tn} \quad \text{(S12)}$$

Supporting Results

Predicted degradation rates and relative contributions of each short-lived reactive intermediates to the overall photodegradation are provided in Table S4. The prediction generally fitted with the observation of a systematic decrease in degradation rates in the presence of DOM, although predicted values of absolute degradation rates were more uncertain. The predicted degradation rates proved extremely sensitive to the average path length while the relative contribution of each photodegradation processes was left completely unaffected by this parameter. The best fit to experimental data was obtained with an average path length of 8 cm (relatively lower than the actual value estimated at 15 cm). Predicted data were only compared with each other. Note that k_{dir} was not computed and that we used the observed values of degradation rates in UW instead. Indeed, k_{dir} strongly depends on the experimental setup, as shown by the wide range of reaction quantum yield for direct photodegradation gathered in Zeng et al.[10] for atrazine and *S*-metolachlor with different light sources.

Table S5 Comparison of predicted and observed degradation rates and presentation of the predicted contribution of each short-lived reactive intermediate to the overall photodegradation.

		predicted contribution (%)				k_{deg} (d^{-1})		obs / pred
pesticide	condition	direct	HO•	$^1O_2$	$^3DOM^*$	obs	pred	(%)
atrazine	DIR	100	0	0	0	0.57	0.57	100
	NIT	25	75	0	0	0.46	0.94	58
	SRFA	34	22	2	42	0.14	0.12	164
	TOT	17	62	1	20	0.3	0.15	144
S- metolachlor	DIR	100	0	0	0	0.28	0.28	100
	NIT	5	95	0	0	0.28	5.11	8
	SRFA	8	54	4	33	0.09	0.10	144
	TOT	3	87	1	9	0.11	0.21	74

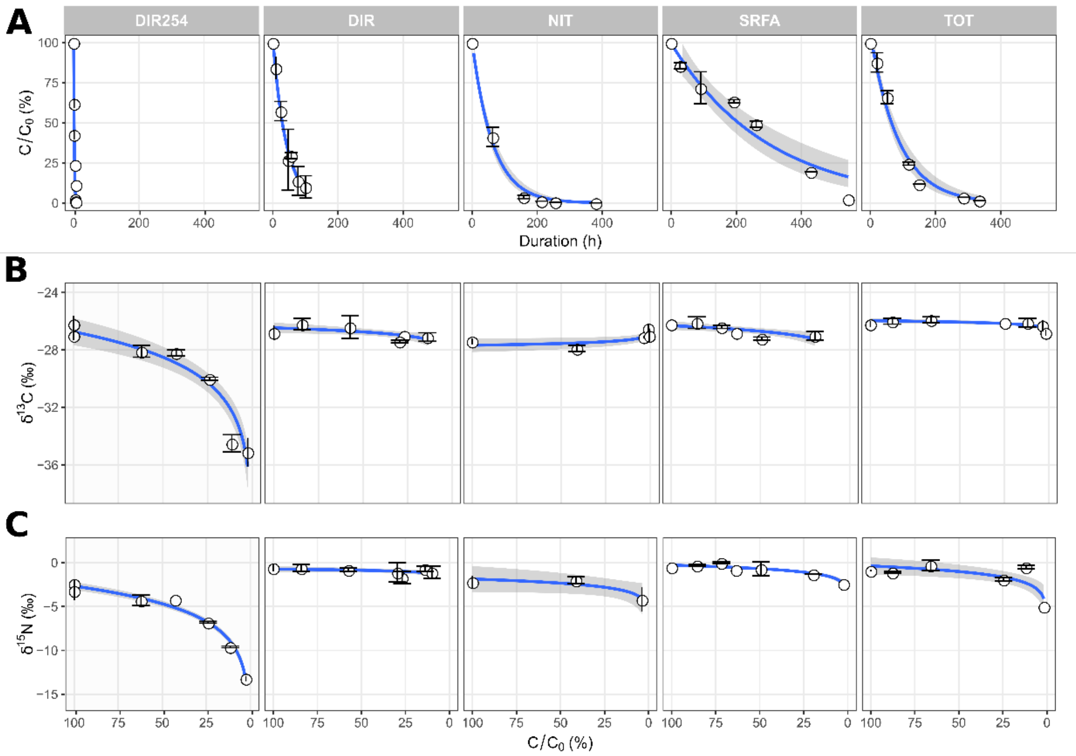

Fig. S5 Observed degradation kinetics (A) and Rayleigh plots for carbon (B) and nitrogen (C) for atrazine.

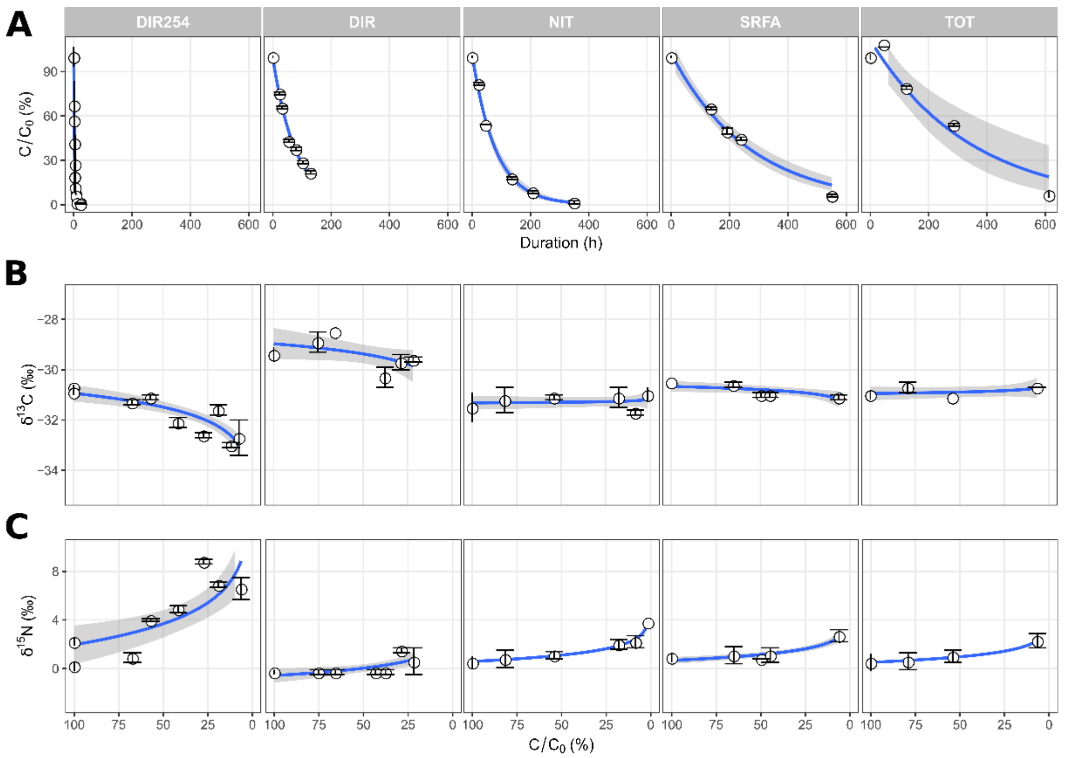

Fig. S6 Observed. degradation kinetics (A) and Rayleigh plots for carbon (B) and nitrogen (C) for *S*-metolachlor.

Supporting References

1. E. J. Smith, W. Davison and J. Hamilton-Taylor, Methods for preparing synthetic freshwaters, *Water Res.*, 2002, **36**, 1286–1296, DOI: 10.1016/S0043-1354(01)00341-4.

2. J. R. Laszakovits, S. M. Berg, B. G. Anderson, J. E. O'Brien, K. H. Wammer and C. M. Sharpless, *p*-nitroanisole/pyridine and *p*-nitroacetophenone/pyridine actinometers revisited: Quantum yield in comparison to ferrioxalate, *Environ. Sci. Technol. Let.*, 2017, **4**, 11–14, DOI: 10.1021/acs.estlett.6b00422.

3. D. Dulin and T. Mill, Development and evaluation of sunlight actinometers, *Environ. Sci. Technol.*, 1982, **16**, 815–820, DOI: 10.1021/es00105a017.

4. R. P. Schwarzenbach, P. M. Gschwend and D. M. Imboden, *Environmental organic chemistry*, John Wiley & Sons, third edn., 2016.

5. J. S. Gaffney, N. A. Marley and M. M. Cunningham, Measurement of the absorption constants for nitrate in water between 270 and 335 nm, *Environ. Sci. Technol.*, 1992, **26**, 207–209, DOI: 10.1021/es00025a027.

6. O. F. Elsayed, E. Maillard, S. Vuilleumier, I. Nijenhuis, H. H. Richnow and G. Imfeld, Using compound-specific isotope analysis to assess the degradation of chloroacetanilide herbicides in lab-scale wetlands, *Chemosphere*, 2014, **99**, 89–95, DOI: 10.1016/j.chemosphere.2013.10.027.

7. C. Olivieri Alejandro, M. Faber Nicolaas, J. Ferré, R. Boqué, H. Kalivas John and H. Mark, Uncertainty estimation and figures of merit for multivariate calibration (IUPAC Technical Report), *Pure Appl. Chem.*, 2006, **78**, 633–661, DOI: 10.1351/pac200678030633.

8. C. Villette, L. Maurer, A. Wanko and D. Heintz, Xenobiotics metabolization in *Salix alba* leaves uncovered by mass spectrometry imaging, *Metabolomics*, 2019, **15**, 122, DOI: 10.1007/s11306-019-1572-8.

9. J. Masbou, G. Drouin, S. Payraudeau and G. Imfeld, Carbon and nitrogen stable isotope fractionation during abiotic hydrolysis of pesticides, *Chemosphere*, 2018, **213**, 368–376, DOI: 10.1016/j.chemosphere.2018.09.056.

10. T. Zeng and W. A. Arnold, Pesticide photolysis in prairie potholes: Probing photosensitized processes, *Environ. Sci. Technol.*, 2013, **47**, 6735–6745, DOI: 10.1021/es3030808.

11. M. Bodrato and D. Vione, APEX (Aqueous Photochemistry of Environmentally occurring Xenobiotics): a free software tool to predict the kinetics of photochemical processes in surface waters, *Environ. Sci. Process. Impacts*, 2014, **16**, 732–740, DOI: 10.1039/C3EM00541K.

12. E. M. L. Janssen, P. R. Erickson and K. McNeill, Dual roles of dissolved organic matter as sensitizer and quencher in the photooxidation of tryptophan, *Environ. Sci. Technol.*, 2014, **48**, 4916–4924, DOI: 10.1021/es500535a.

13. D. Vione, V. Maurino, C. Minero, M. E. Carlotti, S. Chiron and S. Barbati, Modelling the occurrence and reactivity of the carbonate radical in surface freshwater, *Comptes Rendus Chimie*, 2009, **12**, 865–871, DOI: 10.1016/j.crci.2008.09.024.

14. C. K. Remucal, The role of indirect photochemical degradation in the environmental fate of pesticides: A review, *Environ. Sci. Process. Impacts*, 2014, **16**, 628–653, DOI: 10.1039/c3em00549f.

15. P. Westerhoff, S. P. Mezyk, W. J. Cooper and D. Minakata, Electron pulse radiolysis determination of hydroxyl radical rate constants with Suwannee river fulvic acid and other dissolved organic matter isolates, *Environ. Sci. Technol.*, 2007, **41**, 4640–4646, DOI: 10.1021/es062529n.

16. R. M. Cory, J. B. Cotner and K. McNeill, Quantifying interactions between singlet oxygen and aquatic fulvic acids, *Environ. Sci. Technol.*, 2009, **43**, 718–723, DOI: 10.1021/es801847g.

17. M. Schmitt, P. R. Erickson and K. McNeill, Triplet-state dissolved organic matter quantum yields and lifetimes from direct observation of aromatic amine oxidation, *Environ. Sci. Technol.*, 2017, **51**, 13151–13160, DOI: 10.1021/acs.est.7b03402.

18. G. V. Buxton, C. L. Greenstock, W. P. Helman and A. B. Ross, Critical review of rate constants for reactions of hydrated electrons, hydrogen atoms and hydroxyl radicals ($\cdot OH/\cdot O^-$) in Aqueous Solution, *J. Phys. Chem. Ref. Data*, 1988, **17**, 513–886, DOI: 10.1063/1.555805.

19. E. Appiani, R. Ossola, D. E. Latch, P. R. Erickson and K. McNeill, Aqueous singlet oxygen reaction kinetics of furfuryl alcohol: effect of temperature, pH, and salt content, *Environ. Sci. Process. Impacts*, 2017, **19**, 507–516, DOI: 10.1039/C6EM00646A.

20. M. M. Dong and F. L. Rosario-Ortiz, Photochemical formation of hydroxyl radical from effluent organic matter, *Environ. Sci. Technol.*, 2012, **46**, 3788–3794, DOI: 10.1021/es2043454.

21. K. Cawley, J. Korak and F. Rosario-Ortiz, Quantum yields for the formation of reactive intermediates from dissolved organic matter samples from the Suwannee river, *Environ. Eng. Sci.*, 2015, **32**, 31–37, DOI: 10.1089/ees.2014.0280.

22. J. Wenk, U. von Gunten and S. Canonica, Effect of dissolved organic matter on the transformation of contaminants induced by excited triplet states and the hydroxyl radical, *Environ. Sci. Technol.*, 2011, **45**, 1334–1340, DOI: 10.1021/es102212t.

23. D. Buchner, B. Jin, K. Ebert, M. Rolle, M. Elsner and S. B. Haderlein, Experimental determination of isotope enrichment factors - bias from mass removal by repetitive sampling, *Environ. Sci. Technol.*, 2017, **51**, 1527–1536, DOI: 10.1021/acs.est.6b03689.